Finite-size dynamics of inhibitory and excitatory interacting spiking neurons

Maurizio Mattia and Paolo Del Giudice
Complex System Unit, Technologies and Health Department, Istituto Superiore di Sanità–Viale Regina Elena 299, 00161 Roma, Italy
(Received 9 April 2004; published 23 November 2004)

The dynamic mean-field approach we recently developed is extended to study the dynamics of population emission rates $\nu(t)$ for a finite network of coupled excitatory (E) and inhibitory (I) integrate-and-fire (IF) neurons. The power spectrum of $\nu(t)$ in an asynchronous state is computed and compared to simulations. We calculate the interpopulations transfer functions and show how synaptic interaction modulates the otherwise low-pass filter with resonances which go well beyond the filter's cut ($\omega \sim \nu$), allowing efficient information transmission on very short time scales determined by spike transmission delays. The saddle-node instability of the asynchronous state is studied and a simple exact dependence of the stability condition on the current-to-rate gain functions is derived, by which self-couplings (EE and II) decrease stability while mutual interaction (EI and IE) favor stability.

DOI: 10.1103/PhysRevE.70.052903 PACS number(s): 87.18.Sn, 05.90.+m, 05.40.−a, 87.19.La

Realistic models of interacting spiking neurons must ultimately encompass multiple interacting modules, for which the intermodule and intramodule connectivity pattern and synaptic couplings define the architecture of interest in a specific setting. Even at the crude modeling level of integrate-and-fire (IF) current-driven neurons with instantaneous synaptic input, predicting the dynamical properties of multiple interacting neural populations is a difficult task. It has been increasingly recognized that noisy regimes, in which the collective firing of a population of neurons exhibits important fluctuations, provide a key for the description of biologically relevant dynamic phenomena, e.g., fast collective oscillations with frequencies largely exceeding the single-neuron firing rate [1–3]. The "diffusion approximation" has been widely adopted for the description of the noisy dynamics of a single neuron, or a homogeneous population of IF neurons; a few attempts have dealt so far with multiple populations of interacting IF neurons. In this Brief Report, by extending an approach introduced in [4] to two self- and mutually interacting populations of excitatory and inhibitory neurons, we attempt a further step towards the analytical and quantitative description of biologically interesting architectures. Besides this generic interest, the approach taken here has some implications on the problem of information transmission in complex neural systems [5,6]. It is known that a network of spiking neurons firing asynchronously can encode signals covering a frequency band extending well beyond the emission rate of the individual neurons; in the second part of the present paper, we briefly focus on the "input-output" properties of the neural populations as linear systems characterized by suitable transfer functions: both the intramodule and intermodule synaptic interactions produce resonances in the frequency response, which select optimal bands for the information transmission. The present work illustrates how one can analytically put in relatively simple terms the expected role of synaptic couplings in shaping the signal-to-noise transmission properties.

Before describing the results, we summarize the formalism, referring for details to [4], where we introduced a dynamic, mean-field "emission rate equation" describing the time-dependent firing activity $\nu(t)$ of a finite number of interacting IF neurons in noisy regimes, with a distribution of spike transmission delays and instantaneous synaptic currents.

In the diffusion approximation [7], the stochastic dynamics of an IF neuron's membrane potential is described by the Langevin equation $\dot{V}=f(V)+\mu(V,t)+\sigma(V,t)\Gamma(t)$, where $f(V)$ is the leakage term, and $\mu(V,t)$ and $\sigma^2(V,t)$ are the contributions to the infinitesimal mean and variance of V due to the afferent current. $\Gamma(t)$ is a *white* noise with zero mean and unit variance. The associated Fokker-Planck (FP) equation [8] for the probability $p(v,t)dv$ of having $V(t) \in [v,v+dv]$ is

$$\partial_t p = Lp = \left\{-\partial_v[f(v)+\mu(v,t)] + \tfrac{1}{2}\partial_v^2\sigma^2(v,t)\right\}p.$$

The FP equation is complemented by three boundary conditions for (i) the spike emission when V reaches a threshold θ (absorbing barrier at θ), (ii) the allowed range for V (reflecting barrier in $v_{\min}$, possibly $v_{\min}\to-\infty$), and (iii) the reset of V to a value H after the emission of a spike ("flow conservation" of realizations crossing θ, restarting their random walk from H) [1,4,9–13]. The "probability current" through θ is the number of spikes emitted per unit time and per neuron, the *population emission rate* $\nu(t)=-1/2\sigma^2(v,t)\partial_v p(v,t)|_{v=\theta}$.

In the *mean-field* approach for a population of IF neurons, one assumes all neurons share the same μ and σ^2, which now depend on time through $\nu(t)$: $\mu(v,t)=\mu(v,\nu(t),t)$ and $\sigma^2(v,t)=\sigma^2(v,\nu(t),t)$ [14]. The FP equation is then nonlinear: $L=L(p)$. To solve it, $p(v,t)$ can be expanded into the time-dependent eigenfunctions $\{\phi_n\}$ of L, $L|\phi_n\rangle=\lambda_n|\phi_n\rangle$ with eigenvalues λ_n, and the dynamics of the coefficients a_n of the expansion can be computed as [12] $\dot{a}_n=\lambda_n a_n+\dot{\nu}\Sigma_m a_m\langle\partial_\nu\psi_n|\phi_m\rangle$, where $\{\psi_n\}$ are the eigenfunctions of the adjoint operator $L^+\neq L$. In [4], we used the above equation for a_n to derive an evolution equation for $\nu(t)$ in closed form: (i) "closing the loop" by expressing $\nu(t)$ in terms of $\{a_n\}$ and $\{f_n\}$, and singling out the static mode ($\lambda_0=0$ and $a_0=1$, $Lp=0$), to highlight the role of the static current-to-rate gain function $\Phi(\mu,\sigma)$ (providing the emission frequency of a neuron with stationary input current); (ii) including finite-size effects to describe populations with a finite number N of neurons. Besides incoherent fluctuations (e.g., due to quenched randomness in the neurons' connectivity and/or to external input), which are taken into account in σ^2, finite N corrections arise because (i) for finite but large N, the spiking activity $\nu_N(t)$ fluctuates around $\nu(t)$: $\nu_N(t) \simeq \nu(t) + \sqrt{\nu(t)/N}\gamma(t) \equiv \nu(t) + \eta(t)$, where $\gamma(t)$ is a white noise with zero mean and unit variance; μ and σ^2 become stochastic, and so is the finite-N FP equation [1]; (ii) furthermore, the finite number of neurons has to be explicitly taken into account in the boundary condition expressing the conservation of the exact number of realizations crossing θ and reappearing at H [4]. The resulting "emission rate equation" is

$$\dot{\vec{a}} = (\mathbf{\Lambda} + \mathbf{C}\,\dot{\nu}_N)\vec{a} + \vec{c}\,\dot{\nu}_N + \vec{\psi}\eta,$$

$$\nu_N = \Phi + \vec{f} \cdot \vec{a} + \eta, \qquad (1)$$

where $\vec{a}$ is the vector of the expansion coefficients; the elements of $\vec{f}$ are $f_n = -\frac{1}{2}\partial_v \sigma^2(v,t)\phi_n(v,t)|_{v=\theta}$; the elements of $\vec{c}$ are the coupling terms between the nth mode and the stationary one $c_n = \langle \partial_\nu \psi_n | \phi_0 \rangle$, while $\mathbf{C}$ is the matrix of the coupling terms between the nonstationary modes $C_{nm} = \langle \partial_\nu \psi_n | \phi_m \rangle$; $\Lambda_{nm} = \lambda_n \delta_{nm}$; $n, m \neq 0$ everywhere. The elements of $\vec{\psi}$ are evaluated at the reset potential, $\psi_n(H,t)$. $\eta(t)$ acts as an "endogenous" finite-size noise. Synaptic couplings enter Φ, $\mathbf{C}$, and $\vec{c}$, the latter two being 0 for uncoupled neurons.

In [4] we sketched the derivation of the exact rate equation for multiple, infinite interacting populations. In what follows, we first give the linearized equation for the asynchronous state of coupled excitatory and inhibitory neurons including finite-size effects and then (i) compute the power spectrum of ν_N, (ii) discuss the condition for stability, and (iii) work out the inter-population (infinite-N) transfer functions.

The local analysis is performed around the fixed points determined in the limit $N_x \to \infty$ by the self-consistency equation $\nu_{x0} = \Phi_x(\nu_{E0}, \nu_{I0})$ and $\vec{a}_x = 0$. From now on, x is E for excitatory and I for inhibitory, and $\nu_x(t)$ will denote the first-order displacement of the emission rate of the population x from the fixed point ν_{x0} (subscript N will be omitted). The linearized emission rate equation is then

$$\dot{\vec{a}}_x(t) = \mathbf{\Lambda}_x \vec{a}_x(t) + \sum_{y=E,I} \vec{c}_{xy}\dot{\nu}_y(t-\delta) + \vec{\psi}_x \eta_x(t),$$

$$\nu_x(t) = \sum_{y=E,I} \Phi'_{xy}\nu_y(t-\delta) + \vec{f}_x \cdot \vec{a}_x(t) + \eta_x(t), \qquad (2)$$

where $\Phi'_{xy} \equiv \partial \Phi_x / \partial \nu_y$, $\vec{c}_{xy} = \langle \partial_{\nu_y} \vec{\psi}_x | \Phi_{x0} \rangle$ $\eta_x(t)$ is the finite-size white noise with zero mean and variance ν_{x0}/N_x, and all the constant terms $\mathbf{\Lambda}_x$, $\vec{c}_{xy}$, $\vec{\psi}_x$, Φ'_{xy}, and $\vec{f}_x$ are evaluated at the fixed point ν_{x0}. In Eq. (2), only one spike transmission delay δ is considered. In what follows, a distribution $\rho_{xy}(\delta)$ of delays in the transmission of spikes from population y to x is taken into account, substituting in Eq. (2) $\nu_y(t-\delta)$ with $\int_0^\infty \nu_y(t-\delta)\rho_{xy}(\delta)d\delta$ [1,15].

The spectral properties of the asynchronous states can be conveniently probed using the finite-N fluctuations of $\nu_x(t)$, with no need of external oscillatory input. From Eq. (2), the Fourier transform of the emission rate is $\nu_x(\omega) = D_{xx}(\omega)\nu_x(\omega) + D_{xy}(\omega)\nu_y(\omega) + U_x(\omega)\eta_x(\omega)$. $D_{xy}(\omega)$ are the transfer functions, in the frequency domain, characterizing the $y \to x$ transmission properties in the presence of recurrent and mutual interactions, and when $N_x \to \infty$,

$$D_{xy}(\omega) = [\Phi'_{xy} + i\vec{f}_x \cdot (i\omega\mathbf{I} - \mathbf{\Lambda}_x)^{-1}\vec{c}_{xy}\omega]\rho_{xy}(\omega), \qquad (3)$$

where $\rho_{xy}(\omega)$ is the Fourier transform of $\rho_{xy}(\delta)$. In general, the wider $\rho_{xy}(\delta)$ is, the more the high-frequency components of the input signal are damped making the asynchronous states more stable [1,15]. The endogenous noise is transmitted by $U_x(\omega) = 1 + \vec{f}_x \cdot (i\omega\mathbf{I} - \mathbf{\Lambda}_x)^{-1}\vec{\psi}_x$. The power spectrum $P_x(\omega) = |\nu_x(\omega)|^2$ is then

$$P_x(\omega) = \frac{|[1 - D_{yy}(\omega)]U_x(\omega)|^2 \dfrac{\nu_{x0}}{N_x} + |D_{xy}(\omega)U_y(\omega)|^2 \dfrac{\nu_{y0}}{N_y}}{|[1 - D_{xx}(\omega)][1 - D_{yy}(\omega)] - D_{xy}(\omega)D_{yx}(\omega)|^2}. \qquad (4)$$

When the synaptic couplings vanish, and each population forms a set of independent realizations of the same process, both Φ'_{xy} and $\vec{c}_{xy}$ vanish and $D_{xy}(\omega) = 0$, so that $P_x(\omega) = |U_x(\omega)|^2 \nu_{x0}/N_x$. At first order in ν_x, $|U_x(\omega)|^2 = 1 + 2\mathrm{Re}[\vec{f}_x \cdot (i\omega\mathbf{I} - \mathbf{\Lambda}_x)^{-1}\vec{\psi}_x]$.

$P_x(\omega)$ is plotted in Fig. 1, showing a remarkable agreement between theory and simulations. The model neuron used is the VLSI integrate-and-fire neuron (VIF) introduced in [9] with $v_{\min} = H = 0$ and a constant decay term $[f(V) = -\beta]$. Collective behavior of interacting VIFs has been shown to be similar to that of other IF neurons [4,9]. The figure shows a rich pattern of peaks for the stationary asynchronous state. The resonance at $\nu_{E0} = 10$ Hz is due to the small-noise firing of the excitatory neurons: random clusters of neurons starting from similar initial conditions evolve together in a quasideterministic way, providing quasiperiodic bumps of activity at the same frequency as the single neuron firing rate, given by $\mathrm{Im}\lambda_n/2\pi$ [4,5,16]. The 10 Hz resonance in $P_E(\omega)$ is "transmitted" to $P_I(\omega)$, as discussed below. Peaks at higher frequencies $\omega \sim \pi n/\delta$ are due to the transmission delays δ_{xy}, and as such are a manifestation of the interaction among neurons: in the case shown, such resonances are merged because of the "interference" between the modes of the two populations.

When asynchronous states get destabilized, the network can jump to different attractors, including oscillatory states via Hopf-like bifurcations [2]. In what follows, we concentrate on the saddle-node bifurcation occurring when the real poles of the Laplace transform $\nu_x(s)$ of $\nu_x(t)$ cross the imaginary axis. The poles of $\nu_x(s)$ are the solutions of $[1 - D_{xx}(s)][1 - D_{yy}(s)] - D_{xy}(s)D_{yx}(s) = 0$, where $\omega \to -is$ in Eq. (3) to get $D_{xy}(s)$. The bifurcation point is found locating the leading (real) pole in the neighborhood of the origin in the

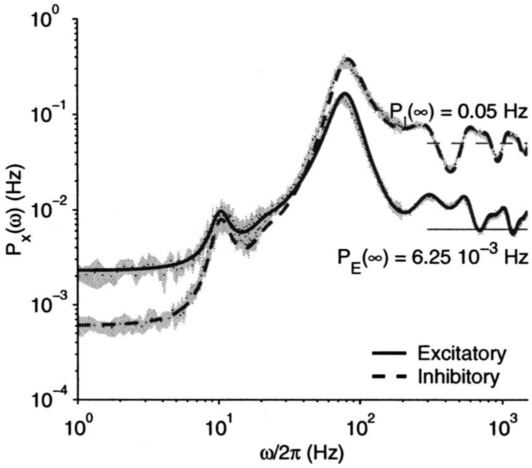

FIG. 1. Power spectra $P_x(\omega)$ for coupled excitatory and inhibitory populations in an asynchronous state: theory vs simulations. The network is composed of $N_E=1600$ excitatory and $N_I=400$ inhibitory VIF (see text) neurons firing on average at $\nu_{E0}=10$ Hz and $\nu_{I0}=20$ Hz. The synaptic conductances are constant: $J_{EE}=0.005$, $J_{EI}=-0.0051$, $J_{IE}=0.028$, and $J_{II}=-0.01$. All spikes are transmitted with a delay $\delta=2$ ms. Excitatory neurons are in a low-noise regime: $(f+\mu)/\sigma^2=18.2 \gg 1$, while the inhibitory ones are in a noisy regime with low $(f+\mu)/\sigma^2=0.6$. Dotted lines are the estimated power spectra from a simulation lasting 10 min: gray strips are their standard errors. Thick solid and dashed lines are, respectively, $P_E(\omega)$ and $P_I(\omega)$ from Eq. (4): the first 256 pairs of eigenmodes are used. Solid and dashed horizontal lines correspond to $P_x(\infty)=\nu_{x0}/N_x$. The membrane potential is measured in units of θ.

complex s plane, where the following expression holds: $D_{xy}(s)=\Phi'_{xy}+(\vec{f}_x\cdot\mathbf{\Lambda}_x^{-1}\vec{c}_{xy}-\Phi'_{xy}\langle\delta\rangle)s+O(s^2)$. $\langle\delta\rangle$ is the average transmission delay. The real pole can be computed from the resulting linear equation: $s_0 \propto (1-\Phi'_{EE})(1-\Phi'_{II})-\Phi'_{EI}\Phi'_{IE}$. The stability boundary is $s_0=0$ so that the asynchronous state will be stable with respect to the saddle-node bifurcations if

$$\Phi'_{EE} < 1 + \frac{|\Phi'_{EI}|\Phi'_{IE}}{1+|\Phi'_{II}|}. \tag{5}$$

($\Phi'_{xI}\leqslant 0$ and $\Phi'_{xE}\geqslant 0$ because increasing inhibition decreases the emission rate.) From the exact condition Eq. (5) it clearly emerges that increasing the excitatory-inhibitory interaction widens the stability region $\mathrm{Re}\, s_0<0$ (in agreement with [2,17]), while high self-couplings favor instability. If one of the mutual interactions vanishes, the exact stability condition for the excitatory population is obtained [4].

The transfer properties of a population of neurons y can be studied in a feed-forward configuration in which the output of the system $\nu_y(t)$ results as the "processing" of the input $\nu_x(t)$ in the absence of feedback $[D_{xy}(\omega)=0]$. We neglect the endogenous noise, assuming $N_y\to\infty$, and the transfer function $T_{yx}(\omega)$ is

$$T_{yx}(\omega) \equiv \frac{\nu_y(\omega)}{\nu_x(\omega)} = \frac{D_{yx}(\omega)}{1-D_{yy}(\omega)}. \tag{6}$$

The denominator is an expression of the self-interaction, which makes $T_{yx}(\omega)$ different in principle from the uncoupled case discussed in [5,18,19].

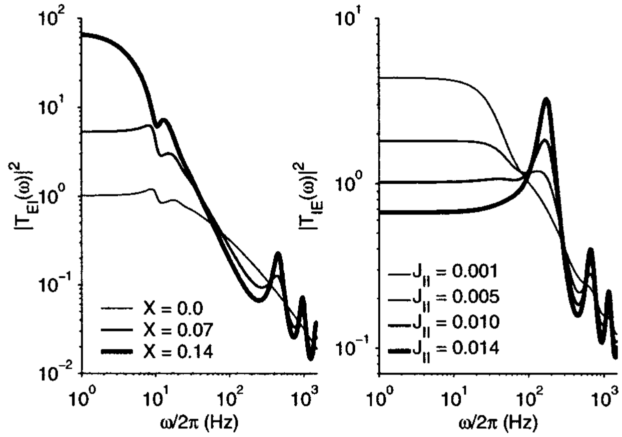

FIG. 2. Theoretical predictions from Eq. (6) for T_{EI} (T_{IE}). Left panel: $|T_{EI}|^2$ for varying relative weights X of the recurrent and external excitatory input (equivalent to changing J_{EE} for fixed ν_{E0}). Right panel: $|T_{IE}|^2$ for varying self-coupling J_{II} and fixed ν_{I0}. J_{II} are measured in units of θ.

Figure 2 shows $|T_{yx}(\omega)|^2$ from Eq. (6) for varying intensities of the recurrent y-y interaction, with parameters chosen such that ν_{y0} is the same for all cases. The population transfer functions are low-pass filters, modulated by resonances related both to the self-interaction and to the amount of fluctuations in the neural activity. The left panel in Fig. 2 shows T_{EI}: the excitatory population is in a low-noise regime, which shows up in the low-ω modulation ($\omega\sim\nu_{E0}=10$ Hz); the latter would correspond to a "diffusion" ripple in $P_E(\omega)$, which is actually obscured by the overwhelming peak around $\lambda \sim \nu_{E0}$ due to the finite-size effects, analogous to the one appearing in Fig. 1. For the uncoupled case ($X\equiv\mu_E/\mu_{\mathrm{ext}}=0$), the only modulation is the low-ω ripple, while more and more prominent peaks appear for increasing self-excitation, at $\omega\sim 2\pi n/\delta$ [imaginary parts of the δ-related "transmission" poles of $\nu_E(s)$ [4]]. The $n=0$ (real) pole contributes the greatest power to $|T_{EI}(0)|^2$. $|T_{IE}|^2$ is shown in the right panel. The inhibitory population is in a noisy regime, and ripples around $\nu_{I0}=20$ Hz do not appear: the uncoupled network would act as a pure low-pass filter with a cut at ν_{I0}. Transmission peaks are now shifted to $\omega\sim(2n+1)\pi/2\delta$.

The coupling-dependent resonances endow the population with nontrivial transmission properties well beyond the low-pass cut. In particular, this implies that the population can react to its input on time scales much shorter than the single-neuron analysis might suggest.

For $\omega\to\infty$, $|T_{yx}|\to$const, $\arg(T_{yx})\to 0$, as known from previous studies [19], for periodic modulation of both the mean and the variance of the input current, which applies in the case shown. We also checked that upon modulating only the mean current the limit $(|T_{yx}|\to 1/\sqrt{\omega})$ [5,18] is recovered.

Without attempting an extensive coverage of related works, we summarize below some relevant previous results on the analysis of interacting excitatory and inhibitory IF neurons, and then list the main features characterizing the present work. Reference [10] reports a detailed analysis for the dynamics of mean emission rates of (adaptive) leaky IF neurons, for the case of negligible noise in the afferent currents, with an emphasis on the spectrum of characteristic relaxation times towards a supposedly stable asynchronous state; the restriction of the present analysis to the almost deterministic case (without adaptation) is consistent with the results of [10]. The authors of [17], restricting also to the quasideterministic case, and for the "quadratic" IF neuron, work out in detail the stability conditions of the asynchronous state; as far as the dependence on the synaptic couplings is concerned, the stability condition derived in [17] for the saddle-node instability is consistent with the general condition (5). In [2], the treatment of two coupled populations of leaky IF neurons covers both the noisy and noiseless case; finite-size effects are incorporated as a stochastic modulation of the mean afferent current; through an extension of the theory developed in [1], the repertoire of available collective states is exposed via numerical analysis, by choosing suitable sections of the system's phase space, and tracing the stability boundaries separating the various regimes of collective activity, for which the relevant quantities (e.g., the frequency of collective oscillations) are extracted. For a simplified architecture, the high-frequency resonances in the power spectrum of the collective activity are shown to be well described by the finite-size theory.

Besides providing, we believe, a unified treatment of previously scattered results on quasideterministic and noisy regimes, new contributions of the present paper include extended treatment of the finite-size effects, which allows a very detailed description of the power spectrum of ν (with an excellent agreement with simulations also for low frequencies) and its use as a self-stimulation of the network to study the frequency response of the system; an emphasis is put on the validity of the approach for a wide class of IF neurons. In particular, the dependence of the stability condition (5) on the synaptic couplings, the general expressions (3) and (4) for the transfer functions, and the power spectrum, with the associated pattern of resonances, do not depend on the details of the IF model, including conductance-based input.

The dependence of the saddle-node stability condition on the synaptic couplings was derived analytically in the form of simple expressions involving the current-to-rate gain functions. This is particularly interesting in view of recent research showing that the gain function of IF neurons fits well *in vitro* experimental data for the firing of pyramidal neurons with noisy input currents [20].

This work has been supported by the ALAVLSI EU Grant No. IST-2001-38099.

[1] N. Brunel and V. Hakim, Neural Comput. **11**, 1621 (1999).

[2] N. Brunel, J. Comput. Neurosci. **8**, 183 (2000).

[3] W. Gerstner, Neural Comput. **12**, 43 (2000).

[4] M. Mattia and P. Del Giudice, Phys. Rev. E **66**, 051917 (2002).

[5] R. B. Stein, A. S. French, and A. V. Holden, Biophys. J. **12**, 295 (1972).

[6] D. J. Mar, C. C. Chow, W. Gerstner, R. W. Adams, and J. J. Collins, Proc. Natl. Acad. Sci. U.S.A. **96**, 10450 (1999); M. J. Chacron, B. Lindner, and A. Longtin, Phys. Rev. Lett. **92**, 080601 (2004).

[7] H. C. Tuckwell, *Introduction to Theoretical Neurobiology* (Cambridge University Press, Cambridge, 1988), Vol. 2.

[8] H. Risken, *The Fokker-Planck Equation: Methods of Solution and Applications* (Springer-Verlag, Berlin, 1984).

[9] S. Fusi and M. Mattia, Neural Comput. **11**, 633 (1999).

[10] A. Treves, Network **4**, 259 (1993).

[11] L. F. Abbott and C. van Vreeswijk, Phys. Rev. E **48**, 1483 (1993).

[12] B. W. Knight, D. Manin, and L. Sirovich, in *Proceedings of SRC, Lille-France*, edited by E. C. Gerf (1996).

[13] B. W. Knight, Neural Comput. **12**, 473 (2000).

[14] D. J. Amit and N. Brunel, Cereb. Cortex **7**, 237 (1997a).

[15] M. Mattia and P. Del Giudice, Sci. Math. Japonicae **18**, 335 (2003).

[16] B. W. Knight, J. Gen. Physiol. **59**, 734 (1972); M. Spiridon and W. Gerstner, Network **10**, 257 (1999); N. Hohn and A. N. Burkitt, Phys. Rev. E **63**, 031902 (2001); B. Lindner, L. Schimansky-Geier, and A. Longtin, *ibid.* **66**, 031916 (2002).

[17] D. Hansel and G. Mato, Phys. Rev. Lett. **86**, 4175 (2001); D. Hansel and G. Mato, Neural Comput. **15**, 1 (2003).

[18] N. Brunel, F. S. Chance, N. Fourcaud, and L. F. Abbott, Phys. Rev. Lett. **86**, 2186 (2001).

[19] B. Lindner and L. Schimansky-Geier, Phys. Rev. Lett. **86**, 2934 (2001).

[20] A. Rauch, G. La Camera, H.-R. Lüscher, W. Senn, and S. Fusi, J. Neurophysiol. **90**, 1598 (2003); M. Giugliano, P. Darbon, M. Arsiero, H.-R. Lüscher, and J. Streit, *ibid.* **92**, 977 (2004).